



## Rapid Communication

## Microstructure and properties of spark plasma sintered Fe–Cr–Mo–Y–B–C bulk metallic glass

Sandip P. Harimkar<sup>a,\*</sup>, Sameer R. Paital<sup>b</sup>, Ashish Singh<sup>a</sup>, Robert Aalund<sup>c</sup>, Narendra B. Dahotre<sup>b</sup><sup>a</sup> School of Mechanical and Aerospace Engineering, Oklahoma State University, Stillwater, OK 74078, United States<sup>b</sup> Department of Materials Science and Engineering, The University of Tennessee, Knoxville, TN 37996, United States<sup>c</sup> Thermal Technology LLC, Santa Rosa, CA 95403, United States

## ARTICLE INFO

## Article history:

Received 12 April 2009

Received in revised form 6 July 2009

Available online 10 August 2009

## PACS:

81.05.Kf

81.20.Ev

81.70.Bt

81.05.Pj

## Keyword:

Alloys

## ABSTRACT

Fabrication of Fe-based amorphous alloy using spark plasma sintering (SPS) process has been reported. Fully amorphous compacts with ~95% relative density were successfully sintered at temperature about 100 °C lower than glass transition temperature ( $T_g$ : 575 °C). Formation of crystalline  $\text{Fe}_{23}(\text{C}, \text{B})_6$  phases within near-fully dense (~99%) amorphous matrix is observed at sintering temperatures (>550 °C) close to glass transition temperature. Microstructure evolution in sintered compacts indicated that density, degree of crystallinity, and mechanical properties can be effectively controlled by optimizing SPS parameters.

Published by Elsevier B.V.

## 1. Introduction

Spark plasma sintering (SPS) is rapidly evolving as a flexible process for fabricating traditional difficult-to-sinter materials and novel nanocrystalline/amorphous material (nanoceramics, nanocomposites, bulk metallic glasses and functionally graded materials) [1–4]. By combining the effects of uniaxial pressure and pulsed direct current, the process offers enormous possibilities of fully sintering these materials at significantly lower temperatures and shorter sintering times (less than an hour) compared to conventional hot sintering. While exact nature of sintering mechanism in spark plasma sintering is still being debated, researchers are extending the capabilities of the process to fabricate novel compositions and microstructures [5,6]. The process has been successfully demonstrated for sintering metals/alloys, intermetallics, carbides, nitrides, borides, oxides silicides, and composites [7].

Amorphous materials exhibit excellent properties such as high hardness, elastic modulus/limit, corrosion/wear resistance important in structural applications [8]. Significant progress has been done in understanding the glass forming abilities of various multi-component systems and optimum compositions with glass forming abilities at lower cooling rates have been identified [9]. In spite of excellent properties of the amorphous alloys, actual utilization of

amorphous alloys in structural applications is still limited. Fabrication of large size components of bulk metallic glass using conventional rapid solidification processing route is still a challenge [10]. Since processes of fabrication of amorphous powders are well established, spark plasma sintering presents a unique possibility of fast sintering of amorphous powders into dense compacts and near-net shape components while retaining glassy structure. SPS of various composition of nickel/zirconium-based bulk metallic glass is reported [11,12]. Also reported is the sintering of Fe-based amorphous alloy reinforced with  $\text{Y}_2\text{O}_3$  [13]. While most of these initial reports primarily focused on the phase characterization of the sintered amorphous compacts, detailed investigations on microstructure evolution and mechanical property development are not done. This paper deals with the spark plasma sintering of Fe-based ( $\text{Fe}_{48}\text{Cr}_{15}\text{Mo}_{14}\text{Y}_2\text{C}_{15}\text{B}_6$ ) amorphous powder. Densification behavior and microstructure evolution in compacts fabricated using various spark plasma sintering parameters is characterized and discussed. Also, a brief note on development of mechanical properties especially hardness and indentation fracture toughness of sintered compacts of amorphous alloy is presented.

## 2. Experimental procedure

Fe-based amorphous alloy powder (particle size: <25  $\mu\text{m}$ ) of composition  $\text{Fe}_{48}\text{Cr}_{15}\text{Mo}_{14}\text{Y}_2\text{C}_{15}\text{B}_6$  was used the present investiga-

\* Corresponding author. Tel.: +1 405 744 5830.

E-mail address: [sandip.harimkar@okstate.edu](mailto:sandip.harimkar@okstate.edu) (S.P. Harimkar).

tion. The amorphous powder was prepared by high pressure gas atomization. A mixture of pure elemental powders of Fe, Cr, Mo, Y, B, and C with nominal chemical composition of  $\text{Fe}_{48}\text{Cr}_{15}\text{Mo}_{14}\text{Y}_2\text{C}_{15}\text{B}_6$  was melted under high purity argon atmosphere and then atomized using high purity inert gas. Differential scanning calorimetry (DSC) with a constant heating rate of  $20^\circ\text{C}/\text{min}$  was used to determine the glass transition and crystallization temperature of the as-received amorphous alloy powder. The amorphous powder was sintered in commercial spark plasma sintering unit (Thermal Technology LLC, Santa Rosa, CA). In an attempt to maximize the density and retain the amorphous composition, various combinations of SPS processing parameters (sintering temperature and holding time) were explored. A summary of SPS processing parameters used in present investigations is presented in Table 1. Initial sintering experiments were conducted at  $475^\circ\text{C}$ , the temperature almost  $100^\circ\text{C}$  lower than glass transition temperature to maximize the chances of retaining amorphous compositions. The vertical force of 40 kN was used in all the sintering experiments. The sintering experiments were conducted using a tungsten carbide die with a thermocouple placed inside the wall of the die for temperature measurement. Around 7 g amorphous powder was used to sinter each disc specimen of 15 mm diameter and 10 mm height. Following sintering, density of the discs was determined using Archimedes' principle. X-ray diffraction analysis of the sintered discs was carried out using Philips Norelco X-ray diffractometer operating with  $\text{Cu K}\alpha$  ( $\lambda = 1.54178 \text{ \AA}$ ) radiation at 20 kV and 10 mA. The diffraction angle was varied between  $30^\circ$  and  $70^\circ$   $2\theta$  at a step increment of  $0.02^\circ$   $2\theta$  with a count time of 1 s. In partially crystalline sintered samples, average crystallite size was determined from broadening of primary reflection after stripping  $\text{K}\alpha$ . The characterization of microstructure in the sintered discs was conducted using a scanning electron microscope (S3500, HITACHI™). A microhardness tester (BUEHLER™) was used for measuring hardness by performing indentations at a load of 2.94 N and holding time of 12 s. Fracture toughness ( $K_{\text{IC}}$ ) was obtained using direct crack measurement method. The fracture toughness,  $K_{\text{IC}}$ , is given by [14]:

$$K_{\text{IC}} = 0.016 \left( \frac{E}{H} \right)^{1/2} \frac{P}{c^{3/2}}, \quad (1)$$

where  $E$  is the Young's modulus (GPa),  $H$  is the Vickers hardness (GPa),  $P$  is the applied load (N), and  $c$  is the diagonal crack length (m). The literature value of 200 GPa for the Young's modulus of iron-based amorphous alloys was used for fracture toughness calculations [15]. The fracture toughness was obtained for 10 indentations on each sample, and the average value is reported.

### 3. Results and discussion

DSC scan of the as-received amorphous powder is presented in Fig. 1. The powder exhibited characteristic behavior associated with amorphous materials with distinct glass transition at  $\sim 575^\circ\text{C}$  followed by double exothermic peaks corresponding to crystallization temperatures,  $T_{x1}$  and  $T_{x2}$ . The results confirmed the glassy structure of the alloy powder prior to spark plasma sintering. Fig. 2 presents the XRD patterns obtained from as-received

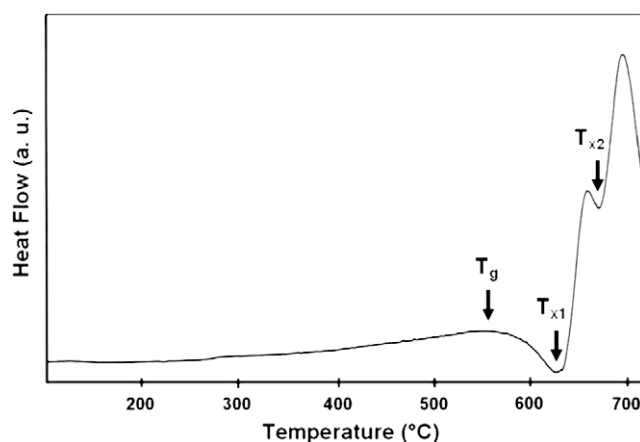


Fig. 1. DSC scan of amorphous  $\text{Fe}_{48}\text{Cr}_{15}\text{Mo}_{14}\text{Y}_2\text{C}_{15}\text{B}_6$ . The arrowheads indicate the glass transition ( $T_g$ ) and crystallization ( $T_{x1}$  and  $T_{x2}$ ) temperatures of the alloy.

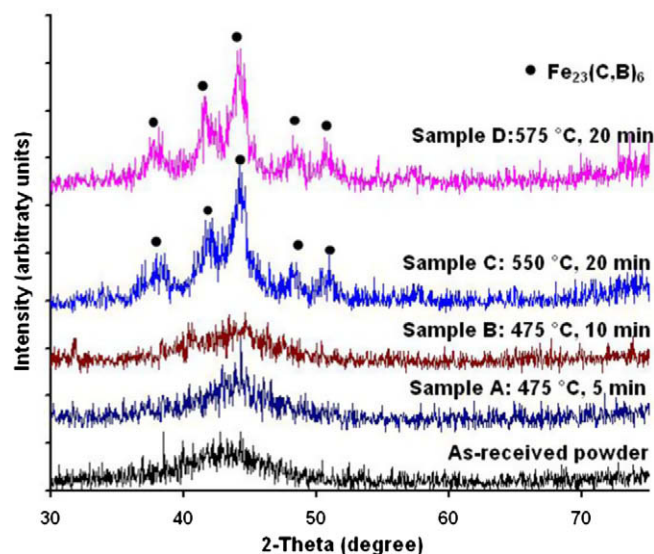


Fig. 2. XRD patterns from Fe-based amorphous powder and compacts spark plasma sintered with various processing parameters.

powder and compacts sintered with various processing parameters (sintering temperature and holding time). The as-received powder exhibits characteristic broad halo with diffused intensity indicating fully amorphous structure. The compacts SPS sintered at temperature lower than glass transition temperature also exhibit fully amorphous structure (samples A and B). To understand the influence of sintering temperature on the phase evolution, two specimens were sintered at temperatures close to glass transition temperature of the amorphous alloy (samples C and D). XRD patterns from these samples exhibit predominantly amorphous background with superimposed crystalline peaks corresponding to  $\text{Fe}_{23}(\text{C}, \text{B})_6$  indicating formation of amorphous matrix embedded with crystalline phases. Table 1 also presents the average crystal-

Table 1  
Summary of SPS processing parameters and properties in sintered compacts.

Sample ID	Sintering temperature ( $^\circ\text{C}$ )	Holding time (min)	Relative density (%)	Crystallite size ( $\text{\AA}$ )	Hardness (HV)	Fracture toughness ( $\text{MPa m}^{1/2}$ )
Sample A	475	5	92.76	–	–	–
Sample B	475	10	94.13	–	–	–
Sample C	550	20	98.96	99	1341	$1.67 \pm 0.3$
Sample D	575	20	99.07	117	1230	$1.58 \pm 0.3$

Download English Version:

<https://daneshyari.com/en/article/1482248>

Download Persian Version:

<https://daneshyari.com/article/1482248>

[Daneshyari.com](https://daneshyari.com)